Trans. JSASS Aerospace Tech. Japan
DOI: 10.2322/tastj.17.127

Drag Reduction on the Basis of the Area Rule of the Small-scale Supersonic Flight Experiment Vehicle Being Developed at Muroran Institute of Technology

By Yuki YAMAZAKI,[1)] Kazuhide MIZOBATA,[2)] and Kazuyuki HIGASHINO [2)]

[1)] *Graduate student, Muroran Institute of Technology, Muroran, Japan*
[2)] *Aerospace Plane Research Center, Muroran Institute of Technology, Muroran, Japan*

(Received June 30th, 2017)

A small-scale supersonic flight experiment vehicle (OWASHI) is being developed at Muroran Institute of Technology as a flying testbed for verification of innovative technologies for high speed atmospheric flights which are essential to next-generation aerospace transportation systems. The second-generation configuration M2011 of the vehicle with a single Air Turbo Ramjet Gas-generator-cycle (ATR-GG) engine has been proposed. Its transonic thrust margin has been predicted to be insufficient, therefore drag reduction in the transonic regime is quite crucial for attainability of supersonic flights. In this study, we propose configuration modifications for drag reduction on the basis of the so-called area rule, and assess their effects through wave drag analysis, wind tunnel tests, and CFD analysis. As a result, the area-rule-based configurations have less drag than the baseline configuration M2011. However, the effects of the proposed bottleneck on the fuselage below the main wing are smaller than predicted. It would be caused by the drag due to separation and shocks around the bottleneck. It is necessary to redesign the area-rule-based bottleneck to be smoother.

Key Words: Supersonic, Drag Reduction, Area Rule, Wave Drag Analysis, Wind Tunnel Test

Nomenclature

AOA	:	angle of attack
$A(x)$	:	the cross-sectional area at x
C_D	:	drag coefficient
$C_{D,0}$	:	zero-lift drag coefficient
C_L	:	lift coefficient
D	:	drag
D_w	:	wave drag of overall vehicle configuration
$D(\theta)$	:	wave drag component due to the Mach plane with a roll angle of θ
L	:	the distance from the nose to the Mach cone origin point or lift
M	:	flight or flow Mach number
S	:	projected area of the cross section
V	:	the body volume
x	:	coordinate along the body axis

1. Introduction

Innovation in technologies for high-speed atmospheric flights is essential for establishment of supersonic/ hypersonic and reusable space transportations. It is quite effective to verify such technologies through small-scale flight tests repeatedly in practical high-speed environments prior to installation to large-scale vehicles. Thus, we are developing a small-scale supersonic flight experiment vehicle as a flying test bed. It has two generations of aerodynamic configuration with a cranked-arrow main wing. In the 1st generation M2006prototype, twin counter-rotating axial fan turbojet (CRAFT) engines[1)] were proposed for propulsion. The aerodynamics and flight capability of the configuration were analyzed through wind-tunnel tests and three-degree-of-freedom flight trajectory calculations.[2)] On the other hand, a revised aerodynamic configuration M2011 has been proposed for the 2nd-generation vehicle with a single Air Turbo Ramjet Gas-Generator-cycle (ATR-GG) engine.[3)] Its wing geometry is quite equivalent to that in the 1st generation but its overall dimension and nose length are enlarged in order to install the ramjet engine and propellants required for supersonic missions. Its transonic thrust margin has been predicted to be insufficient as shown in Fig. 1,[4)] therefore drag reduction in the transonic regime is quite crucial for attainability of supersonic flights.

The so-called *area rule* is believed to be quite effective for such drag reduction. It should be noted that the rule is on the basis of the slender body theory, i.e. a version of the small perturbation theory of compressible flows, at Mach 1.0. Thus it is valid strictly only for slender bodies with very small wings and only at the Mach 1.0 condition. Its applicability to practical winged bodies at other Mach numbers has been assessed through case studies on practical transonic/supersonic vehicles such as YF-102 and Boeing 747 but is not clarified sufficiently. Much more extensive studies are required.

In this study, we aim to reduce transonic drag of the proposed experiment vehicle as well as to assess applicability of the area rule to the practical winged vehicle. To this end we propose design modifications of the vehicle configuration on the basis of the area rule, and analyse their effects through wave drag analysis, wind tunnel tests, and CFD analysis.

J-STAGE Advance published date: January 31st, 2019

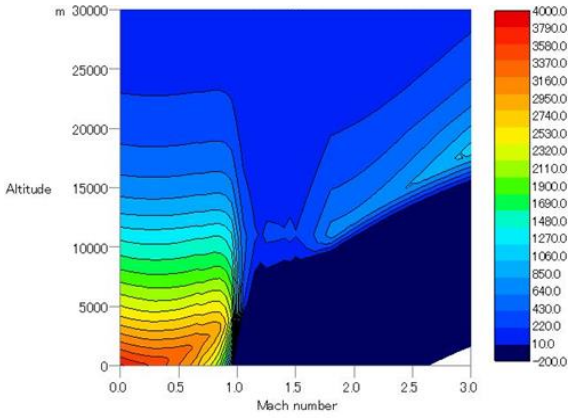

Fig. 1. Thrust margin of the configuration M2011.[4)]

2. The Second-Generation Configuration M2011

A revised aerodynamic configuration M2011 with a single Air Turbo Ramjet Gas-Generator-cycle (ATR-GG) engine is designed as shown in Fig. 2 and Table 1. A diamond wing section of 6% thickness is adopted for reduction of wave drag during supersonic flights. Its main wing has a cranked-arrow planform with an inboard and an outboard leading edge sweepback angles of 66 and 61 degrees, respectively. A high-wing configuration with a dihedral of 1.0 degree is also adopted in order to attain sufficient roll stability. Three types of fuselage length, 5.8m, 6.8m, and 7.8m, are considered tentatively for various quantities of propellants loaded for various missions.

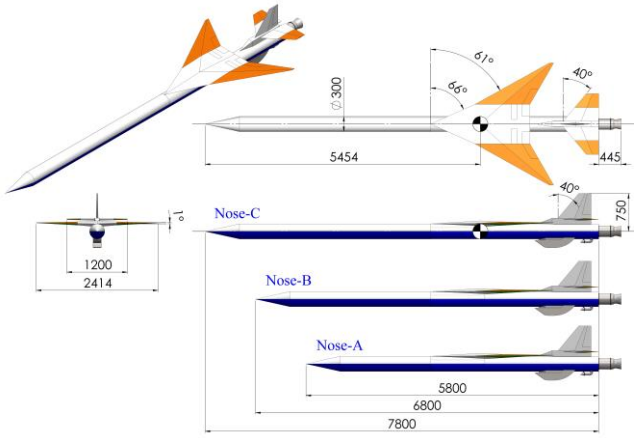

Fig. 2. The proposed revision configuration M2011 for the second generation vehicle design.

Table 1. Dimensions of the configurations M2011.

Wing Span [mm]	2413.5
Wing Area [mm^2]	2148427.8
Fuselage Diameter [mm]	300
Overall Length [mm]	Nose-A: 5800 Propellants 80kg Nose-B: 6800 Propellants 105kg Nose-C: 7800 Propellants 130kg

3. Theory

The area rule was discovered by R. T. Whitcomb[5)] through free-fall experiments of slender bodies with very small wings around sonic conditions. It says that in order to reduce wave drag at Mach 1.0, the cross-sectional area distribution along the body axis should be smoothed. This rule was verified theoretically by Karman's formula on the basis of the slender body theory, i.e. a version of the perturbation theory of compressible flows as follows:

$$D_w = -\frac{\rho V^2}{4\pi}\int_{x_A}^{x_B}\int_{x_A}^{x_B} S''(x_1)S''(x_2)\ln|x_1 - x_2|dx_1dx_2. \quad (1)$$

Here, x is an arbitrary position along the body axis of the vehicle, S is the cross-sectional area of the airframe cut by the Mach plane perpendicular to the body axis. In addition, the optimum cross sectional area distribution was found to be the Sears-Haack curve of Eq. (2). Figure 3 shows the curve in a cubic diagram.

$$A(x) = \frac{16V}{3L\pi}[4x - 4x^2]^{3/2}. \quad (2)$$

Here, x is the nondimensionalized distance from the nose to the cross section $(0 \le x \le 1)$, V is the body volume, and $A(x)$ is the cross-sectional area at x.

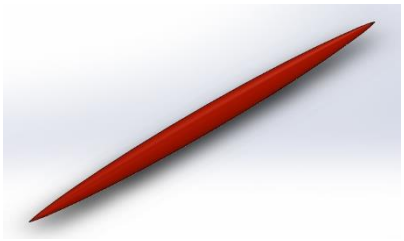

Fig. 3. Sears-Haack body.

The above theory and treatment are valid strictly only for the Mach 1.0 condition. For larger Mach numbers, the Mach planes are no longer perpendicular to the axis. Then R. T. Jones[6)] adopted a superposing or averaging calculation with respect to the roll angle of the Mach plane by intuition as follows:

$$D(\theta) = -\frac{\rho V^2}{4\pi}\int_{x_A(\theta)}^{x_B(\theta)}\int_{x_A(\theta)}^{x_B(\theta)} S''(x_1)S''(x_2)\ln|x_1 - x_2|dx_1dx_2, \quad (3)$$

$$D_w = \frac{1}{2\pi}\int_0^{2\pi} D(\theta)d\theta. \quad (4)$$

Here, S is the projected area of the cross section of the airframe cut by the Mach plane with a roll angle θ. This treatment was applied to the numerical wave drag estimation code WAVEDRAG (NASA Langley Program D 2500).[7)]

Physically speaking, the pressure change in supersonic flow propagates along the surface of the Mach cones. Thus it is also expected by intuition that the wave drag is reduced when the distribution of cross-sectional area of the vehicle cut with Mach cones emanating from an arbitrary point on the body axis is brought close to the Sears-Haack curve.

Thus the area rule has two aspects of uncertainty in its validity and applicability. Firstly, is it applicable to practical

non-slender winged vehicles? Secondly, is it valid at Mach numbers larger than 1.0? Such validity and applicability must be assessed through case studies for practical winged vehicles at various Mach numbers. One of such assessments will be carried out in this study using the proposed supersonic experimental vehicle configuration.

4. The Baseline Configuration M2011 and Area-rule-Based Configurations

The 3D view and the cross-sectional area distribution of the wind tunnel test model of the baseline configuration M2011 are shown in Fig. 4. Compared with the Sears-Haack curve plotted in red, the nose, main wing and tails are protruded.

Modification elements on the basis of the area rule are listed in Table 2 and Fig. 5. The bottleneck has a uniform curvature in order to prevent convergence of compression waves. In addition, the Bulge-B is fatter than the Bulge-A. Six patterns of configuration modifications are proposed by combining these elements. Their 3D views and cross-sectional area distributions are shown in Fig. 6. The design Mach number of these area-rule-based configurations is 1.1.

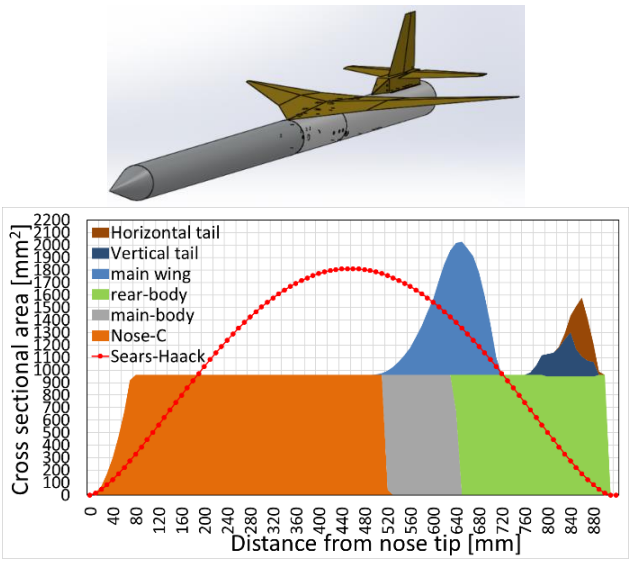

Fig. 4. The wind tunnel test model and its cross-sectional area distribution of the baseline configuration M2011.

Table 2. Modifications on the basis of the area rule.

	Elements	Purpose and effects
Nose cone	ARNose-C	Sharpening the nose to fit the Sears-Haack curve. Reduction of wave drag.
Fuselage	Bottleneck	By narrowing the mid-fuselage around the main wing, the cross-sectional area of the main wing is cancelled. Reduction of wave drag.
	Bulge-A Bulge-B	Relaxation of sudden change in cross sectional area between main wing and tails. Reduction of wave drag. Main landing gear storage. Bulge-B is fatter than Bulge-A
Wing mounting position	Forward-wings	Moving wings forward to fit Sears-Haack curve. Reduction of wave drag. Maintaining the positional relationship between main wing and tails. Maintaining aerodynamic characteristics.

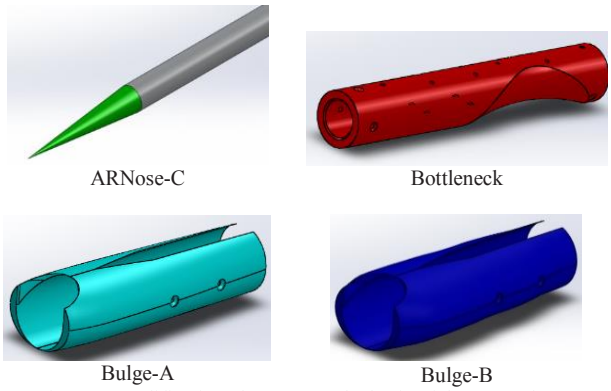

Fig. 5. Modification elements on the basis of the area rule.

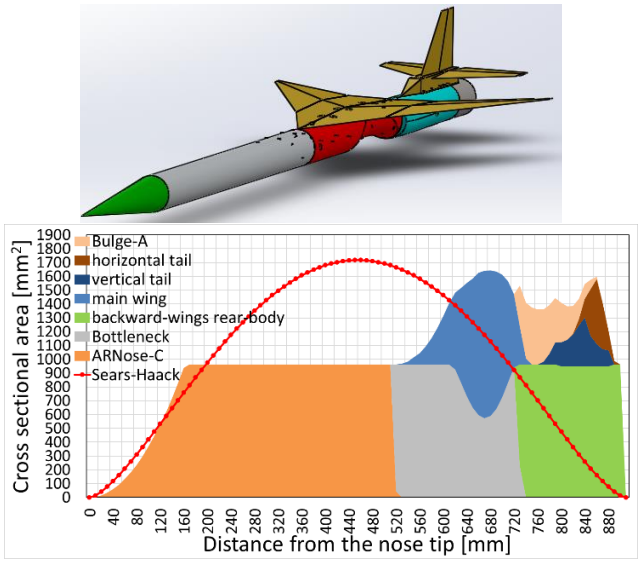

A) The combination of ARNose-C, Bottleneck, Bulge-A, and Backward-wings.

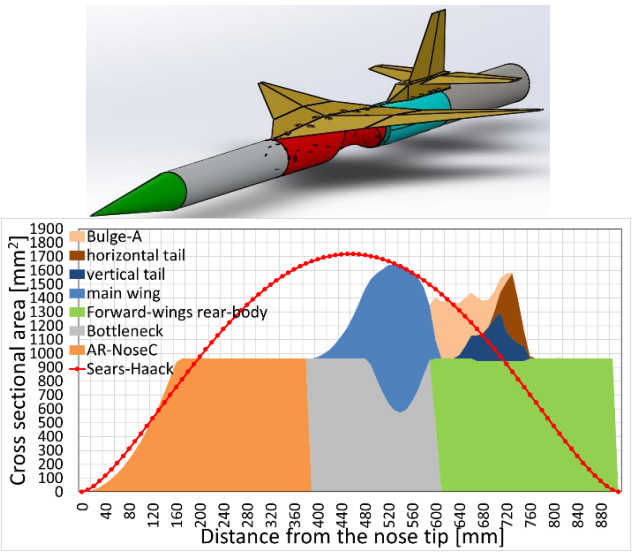

B) The combination of ARNose-C, Bottleneck, Bulge-A, and Forward-wings.

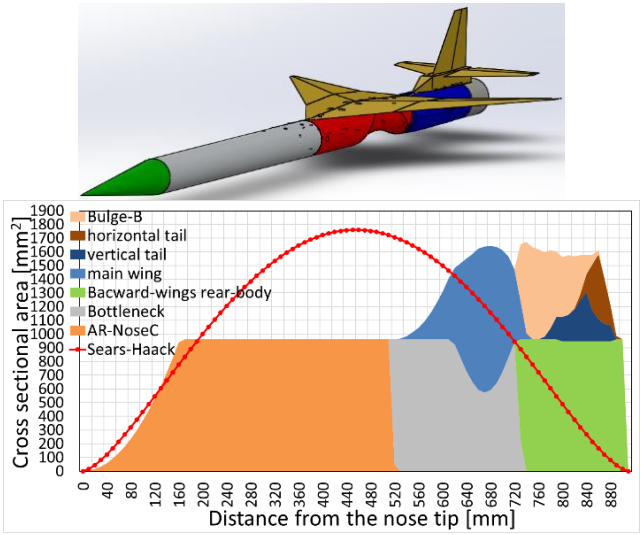

C) The combination of ARNose-C, Bottleneck, Bulge-B, and Backward-wings.

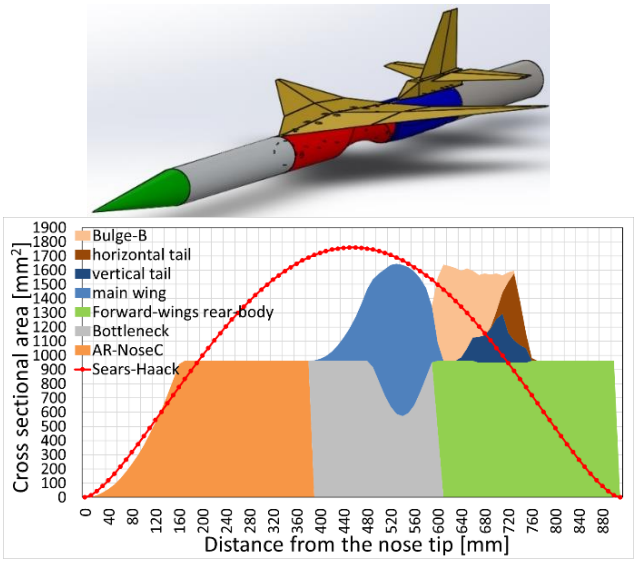

D) The combination of ARNose-C, Bottleneck, Bulge-B, and Forward-wings.

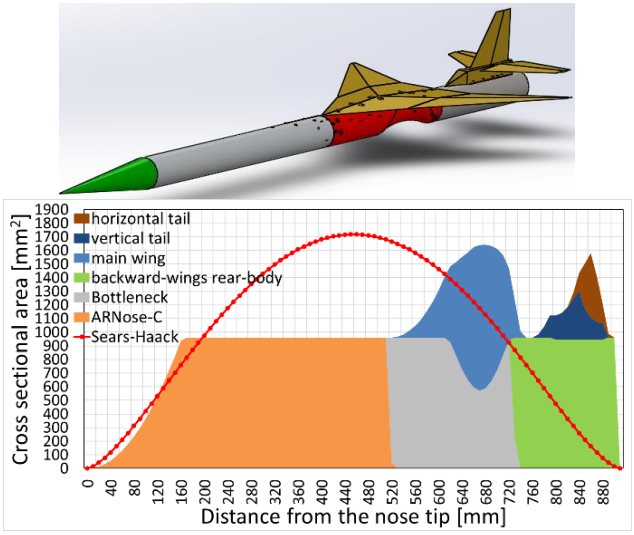

E) The combination of ARNose-C, Bottleneck, and Backward-wings.

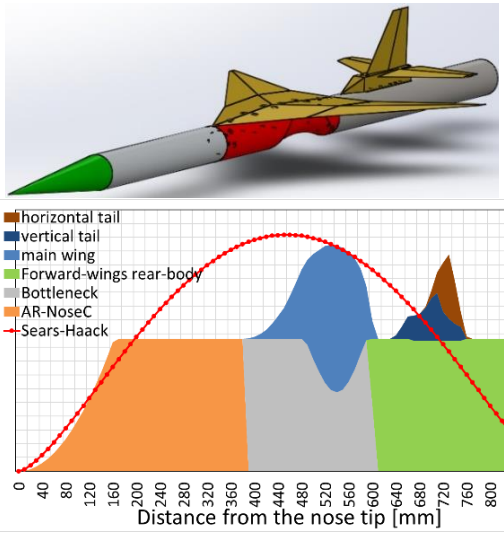

F) The combination of ARNose-C, Bottleneck, and Forward-wings.

Fig. 6. Wind tunnel test models and their cross-section area distributions of area-rule-based configurations.

5. Wave Drag Analysis

In this study, the wave drag of the baseline configuration M2011 and the proposed area-rule-based configurations is estimated and its reduction at Mach numbers above 1.0 is verified before executing the wind tunnel tests. To this end, the wave drag calculation program WAVEDRAG (NASA Langley Program D 2500),[7] is used. It is based on the slender body theory, thus it can handle wave drag only due to relatively weak compression and expansion waves. In this procedure, the wave drag is estimated from Eqs. (3) and (4).

The vehicle configurations to be assessed are 8 patterns, which are the 6 patterns shown in Section 4, the baseline configuration M2011, and the area-rule-based configurations adopting only the area-ruled nose. The results are illustrated in Fig. 7.

Since the design Mach number of the present modification is 1.1, the wave drag of the area-rule-based configurations is significantly smaller than that of the baseline configuration M2011 at Mach 1.1. In addition, all the area-rule-based configurations have smaller wave drag than the baseline up to Mach 1.4. Regarding the effects of bulges, the configurations with Bulge-A and B have succeeded in reducing wave drag at Mach numbers less than 1.2. As for the bottleneck, the wave drag is significantly reduced at Mach numbers between 1.0 and 1.4.

However, since the WAVEDRAG analysis is based on the slender body theory, it cannot estimate the drag due to strong compressions and viscosity. Therefore it is necessary to assess overall drag reduction by wind tunnel tests.

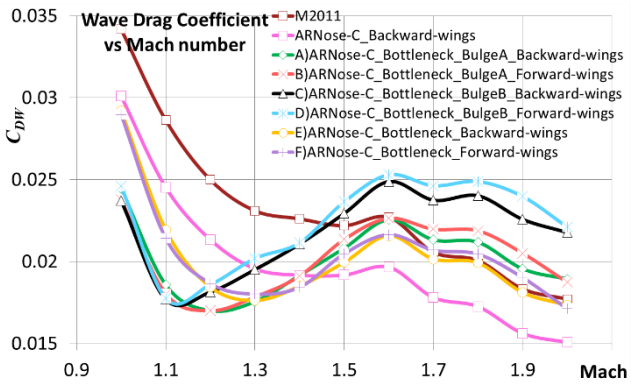

Fig. 7. Results of wavedrag analysis.

6. Wind Tunnel Tests

Wind tunnel tests are carried out using a blowdown-type transonic wind tunnel at JAXA/ISAS to acquire aerodynamic data of the baseline configuration M2011 and the area-rule-based configurations. Aerodynamic forces are measured using a six-component internal balance, and then drag coefficient is estimated. Mach number is 0.7 to 1.3, the angle of attack is -5 to +5 degrees, and the total pressure is 1.5 kgf/cm^2. The overview of the transonic wind tunnel and a vehicle model installation situation are shown in Figs. 8 and 9. The vehicle model is designed and fabricated with a scale reduction ratio of 7/60 to the 2nd generation vehicle, i.e. the wingspan of the model is 28cm. One of the schlieren photos obtained during the wind-tunnel tests is shown in Fig. 10.

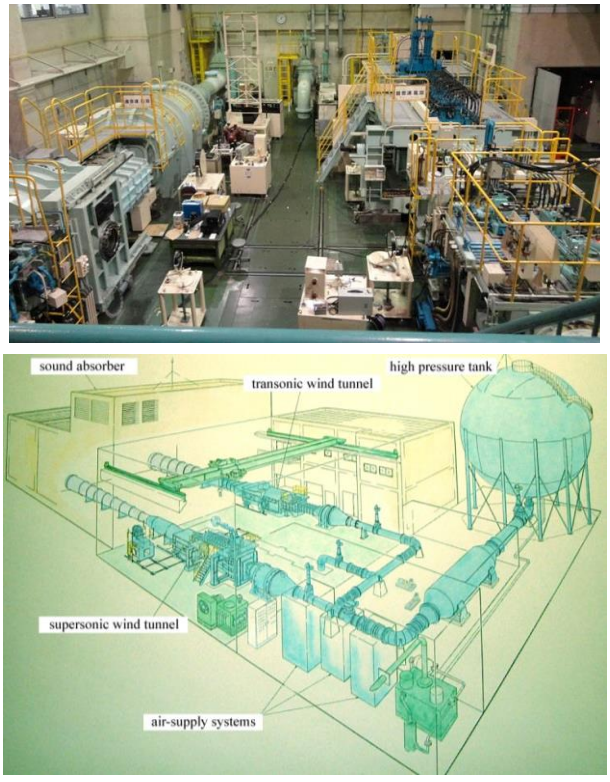

Fig. 8. Overviews of the transonic and supersonic wind tunnels of JAXA/ISAS. The lower schematic view is reproduced from figures in Refs. 8 and 9 on the basis of courtesy of JAXA/ISAS.

Fig. 9. A wing tunnel test model installed in the transonic wind tunnel.

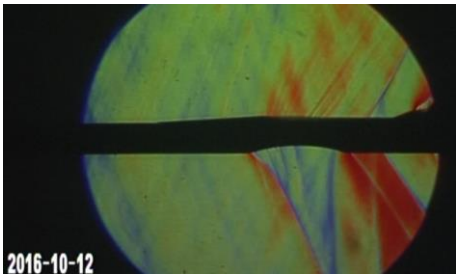

Fig. 10. A schlieren photograph of the wind-tunnel test at M1.1.

The zero-lift drag coefficient $C_{D,0}$ of the wind tunnel test results is shown in Fig. 11. Multiple measurements were carried out for some configurations at some Mach numbers and their results show good reproducibility. On the other hand, some wavy characteristics appear in the transonic regime. They were caused probably by that the Mach waves emanating from the vehicle model reflect on the internal wall of the wind-tunnel and hit the model as shown in the schlieren photo.

As shown in Fig. 11 the area-rule-based configurations have smaller drag than the baseline configuration M2011 at Mach numbers of 1.0 and more. Compared with the pink curve of area-rule-based configuration only with an area-ruled nose, the yellow and green curves with an area-ruled nose, a bottleneck, and a bulge have same amounts of transonic drag. Drag reduction of the bottleneck and the bulge seems to be cancelled by some other effects. Such effects should be investigated through CFD analysis.

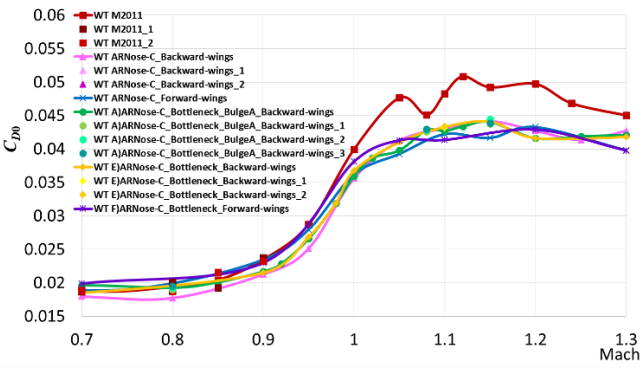

Fig. 11. Results of wind tunnel tests.

7. CFD Analysis

In comparison with the WAVEDRAG analysis, effects of the bottleneck and the bulge in the wind tunnel test results are quite small in drag reduction. The cause is investigated by the following CFD analysis. The main analysis conditions are listed in Table 3. Physical conditions are adjusted to those of wind tunnel tests.

The CFD analysis was carried out for four configurations, the baseline configuration M2011, the area-rule-based configurations only with an area-ruled nose (ARNose-C), that with an area-ruled nose and a bottleneck (ARNose-C_Bottleneck) and that with an area-ruled nose, bottleneck, and a bulge-A (ARNose-C_Bottleneck_BulgeA). Then the zero-lift drag coefficient was evaluated. The results are listed in Tables 4 and 5.

Comparing Table 5 (a), (b) and (c), the pressure drag is increased by the bottleneck, and decreased by the bulge. Since the pressure drag depends on the flow separation and shocks, it is considered that the separation drag and the shock wave drag are increased by the bottleneck. Figure 12 is the comparison between wind-tunnel tests, wave drag estimation, and CFD analysis. The results of wave drag estimation and CFD analysis are shifted vertically and adjusted to the wind-tunnel test results for the baseline configuration M2011 at Mach 1.1 in order to compensate their inability in viscous drag estimation. The wind-tunnel tests and CFD analysis show good agreement, whereas the wave drag estimation disagrees with others. Figure 13 shows the pressure distribution of the area-rule-based configurations. We can see that the pressure is high around the bottleneck because compression waves converge and shocks take place in spite of the uniform curvature of the bottleneck. It is probably because of some displacement effects due to compression-induced separation. It is necessary to redesign the area-rule-based bottleneck to be smoother for prevention of compression wave convergence and further reduction of wave drag.

Table 3. CFD analysis conditions.

Numerical code	ANSYS Fluent
Governing equation	Three-dimensional Navier-Stokes equations
Spatial Discretization	Second-order upwind differencing
Fluid	Air/Ideal-gas
Turbulence model	Spalart-Allmaras
Viscosity model	Sutherland
Mach number	1.1

Table 4. Results of CFD analysis for the baseline configuration M2011.

	Pressure drag	Viscous drag	Total
Drag force [N]	67.69	31.13	98.81
Drag coefficient	0.03884	0.01786	0.05671

Table 5. Results of CFD analysis of the area-rule-based configurations.

(a) The configuration only with an area-ruled nose.

	Pressure drag	Viscous drag	Total
Drag force [N]	60.92	30.57	91.49
Drag coefficient	0.03497	0.01754	0.05251

(b) The configurations with an area-ruled nose and a bottleneck.

	Pressure drag	Viscous drag	Total
Drag force [N]	61.58	29.94	91.52
Drag coefficient	0.03534	0.01718	0.05252

(c) The configuration with an area-ruled nose, a bottleneck, and a bulge-A.

	Pressure drag	Viscous drag	Total
Drag force [N]	60.40	30.01	90.41
Drag coefficient	0.03465	0.01722	0.05187

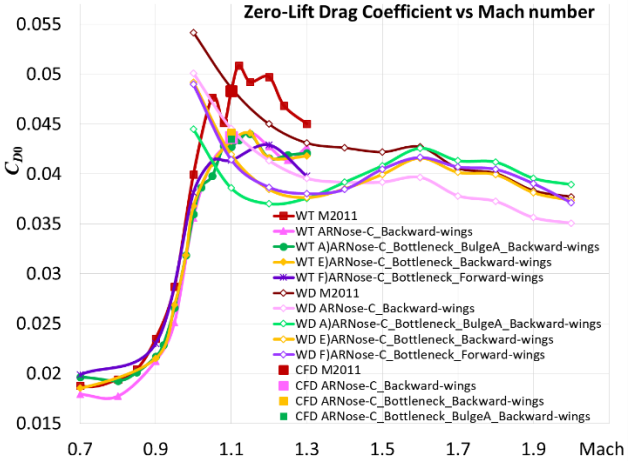

Fig. 12. Comparison between wind-tunnel tests, wave drag estimation, and CFD analysis. The results of wave drag estimation and CFD analysis are shifted vertically and adjusted to the wind-tunnel test results for the baseline configuration M2011 at Mach 1.1.

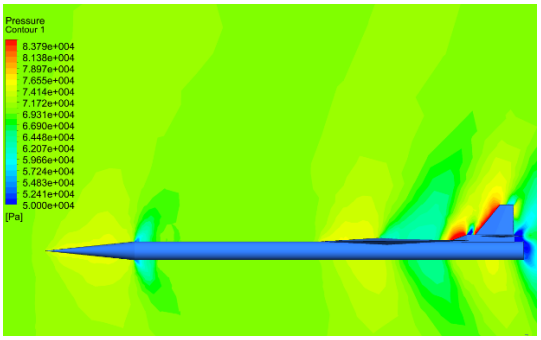

(a) The configuration only with an area-ruled nose.

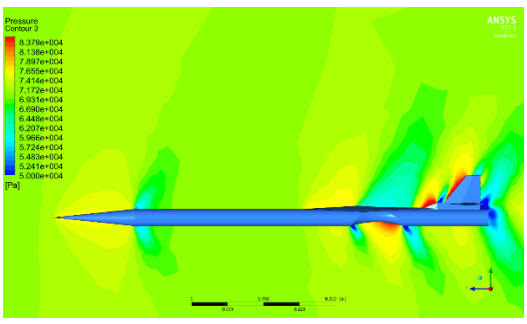

(b) The configuration with an area-ruled nose and a bottleneck.

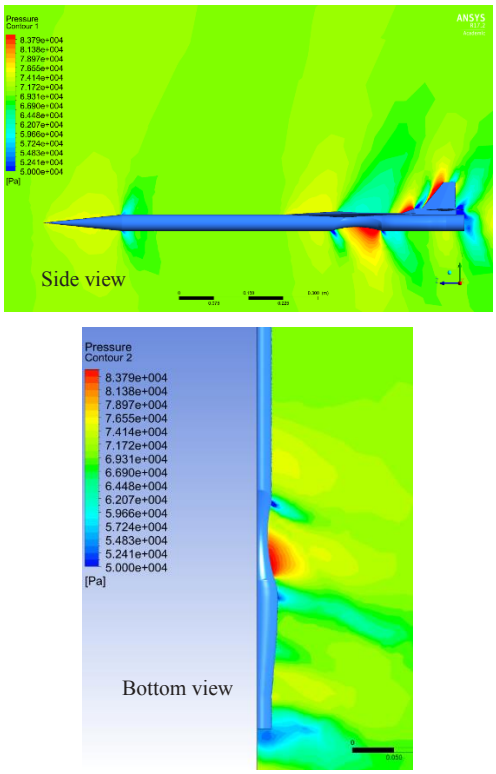

(c) The configuration with an area-ruled nose, a bottleneck, and a bulge-A.

Fig. 13. Results of CFD analysis for pressure distribution around the area-rule-based configurations.

8. Conclusions

A small-scale supersonic flight experiment vehicle (OWASHI) is being developed at Muroran Institute of Technology as a flying testbed for verification of innovative technologies for high speed atmospheric flights which are essential to next-generation aerospace transportation systems. The second-generation configuration M2011 of the vehicle has a single Air Turbo Ramjet Gas-generator-cycle (ATR-GG) engine. Its transonic thrust margin has been predicted to be insufficient, therefore drag reduction in the transonic regime is quite crucial for attainability of supersonic flights. In this study, we proposed configuration modifications for drag reduction on the basis of the so-called area rule, and assessed their effects through wave drag analysis, wind tunnel tests, and CFD analysis. As a result, the area-rule-based configurations have less drag than the baseline configuration M2011. However, the effects of the proposed bottleneck on the fuselage below the main wing were smaller than predicted. It would be caused by the drag due to separation and shocks around the bottleneck. It is necessary to redesign the area-rule-based bottleneck to be smoother.

Acknowledgments

The authors would like to express their sincere gratitude to the Institute of Space and Astronautical Science, Japan Aerospace Exploration Agency, for having provided opportunities of transonic wind-tunnel testing for this research study.

References

1) Minato, R., Kato, D., Higashino, K., and Tanatsugu, N.: Development Study on Counter Rotating Fan Jet Engine for Supersonic Flight, Proceedings of International Symposium on Air Breathing Engines 2011, Goteborg, Sweden, 2011, ISABE-2011-1233.
2) MIZOBATA, K., MINATO, R., HIGUCHI, K., UEBA, M., TAKAGI, S., NAKATA, D., HIGASHINO, K., and TANATSUGU, N.: Development of a Small-scale Supersonic Flight Experiment Vehicle as a Flying Test Bed for Future Space Transportation Research, *Transactions of JSASS, Aerospace Technology Japan*, **12**, ists29 (2014), pp. Po3_1-Po3_10.
3) Minato, R., Higashino, K., and Tanatsugu, N.: Design and Performance Analysis of Bio-Ethanol Fueled GGcycle Air Turbo Ramjet Engine, Proceedings of AIAA Aerospace Science Meeting 2012, Nashville, Tennessee, USA, 2012.
4) MIZOBATA, K., SUZUKI, Y., OOISHI, S., KONDOH, S., ARAI, Y., and HIGASHINO, K.: Aerodynamics and Flight Capability of a Supersonic Flight Experiment Vehicle, *Trans. JSASS Aerospace Tech. Japan*, **14**, ists30 (2016), pp. Pg_1-Pg_8.
5) Whitcomb, R. T.: A Study of the Zero-lift Drag-Rise Characteristics of Wing-Body Configurations Near the Speed of Sound, NACA Rep. 1273, 1956 (Supersedes NACA RM L52H08).
6) Jones, R. T.: Theory of Wing-Body Drag at Supersonic Speeds, NACA Rep. 1284, 1956 (Supersedes NACA RM A53H18a).
7) Craidon, C. B.,: User's Guide for a Computer Program for Calculating the Zero-Lift Wave Drag of Complex Aircraft Configurations, NASA TM-85670, 1983.
8) Funaki, I., Nonaka, S., Yamada, K., and Maru, Y.: Overview of ISAS/JAXA Wind Tunnel Facility, *Aeronautical and Space Sciences Japan*, **64** (2016), pp.199-208 (in Japanese).
9) Wind Tunnel Laboratory of ISAS, http://www.isas.jaxa.jp/home/wtlab/equipment.html (accessed June 30, 2017).